



## **Aerodynamic Analysis of NACA 2412 Airfoil on UAV Aircraft Wing Using Ansys Fluent Software**

**Muhammad Robby<sup>1\*</sup>, Arwizet Karudin<sup>2</sup>, Refdinal<sup>3</sup>, Yolli Fernanda<sup>4</sup>**

<sup>1</sup>Departement Mechanical Engineering Universitas Negeri Padang  
Jalan Prof. Dr. Hamka, Air Tawar, Padang, INDONESIA

<sup>2</sup>Departement Mechanical Engineering Universitas Negeri Padang  
Jalan Prof. Dr. Hamka, Air Tawar, Padang, INDONESIA

<sup>3</sup>Departement Mechanical Engineering Universitas Negeri Padang  
Jalan Prof. Dr. Hamka, Air Tawar, Padang, INDONESIA

<sup>4</sup>Departement Mechanical Engineering Universitas Negeri Padang  
Jalan Prof. Dr. Hamka, Air Tawar, Padang, INDONESIA

\*Corresponding: Muhammad Robby, [mhdrobby809@gmail.com](mailto:mhdrobby809@gmail.com)

*Received 11 November 2024; Accepted 28 Month 2024; Available online 29 November 2024*

### **Abstract**

Technological advances in the era of globalization have increased the demand for unmanned aerial vehicles (UAVs) for various applications, including environmental monitoring, weather research, agriculture, and military needs. The aerodynamic performance of UAVs is highly dependent on wing design, especially airfoils, which play an important role in generating lift and minimizing drag. This research analyzes the aerodynamic performance of the NACA 2412 airfoil on the UAV wing using Computational Fluid Dynamics (CFD) simulation through ANSYS Fluent software. The simulation was conducted with variations in angle of attack and speed to understand the pressure distribution, airflow pattern, and lift (Cl) and drag (Cd) coefficients. The results showed that the optimal angle of attack for the highest Cl/Cd ratio, at 10 m/s and 20 m/s, was 4°, which provided the best aerodynamic efficiency. However, increasing the angle of attack to 20° causes a significant decrease in the Cl/Cd ratio as the drag force increases faster than the lift force, posing a risk of aerodynamic instability. These findings make a significant contribution to designing more efficient and stable UAV wings, supporting the development of more reliable and optimized UAV technologies in the future.

**Keywords:** Aerodynamics, Airfoil, NACA 2412, UAV Wing, ANSYS, CFD

---

### **INTRODUCTION**

Technological advancements in the era of globalization trigger the need for high resource efficiency through automation in various sectors, including in aviation technology. One of the innovations in this field is the unmanned aerial vehicle (UAV), which shows an increasing demand for various applications, such as environmental monitoring, security, meteorological surveillance, weather research, agriculture, mineral exploration, and even military applications [1]. UAVs operate on the principle of aerodynamics to generate lift, enabling autonomous or radio-controlled flight [2].

The main component of a UAV that affects its flying ability is the wing, which consists of airfoils designed to maintain laminar airflow and ensure optimal performance. The wing plays a role in generating the lift that enables the UAV to fly, while the airfoil is an important component in maintaining the balance between lift and drag. The ratio between lift and drag (Cl/Cd) is a key indicator of aerodynamic performance [3], which is calculated using non-dimensional coefficients such as lift (Cl) and drag (Cd) coefficients.

Some popular airfoil types in aviation are Selig, Gottingen, FX Wortmann, and NACA airfoils, each of which has specific characteristics. NACA airfoils, developed by the National Advisory Committee for Aeronautics, have various series used in modern wing design due to their aerodynamic advantages and complete documentation [4]. Among the various NACA types, the NACA 2412 airfoil is a frequently used profile in UAV design due to its simple yet efficient combination of thickness and aerodynamic performance, making it ideal for UAVs that require stability and efficiency over a wide range of speeds [5].

This study aims to analyze the aerodynamic characteristics of NACA airfoil 2412 on a UAV wing by varying the angle of attack and speed using the Computational Fluid Dynamics (CFD) method. CFD simulation through ANSYS Fluent software enables detailed analysis of pressure distribution, airflow patterns, and lift and drag under various flow conditions. Based on the simulations, it was found that the optimal angle of attack for the highest Cl/Cd ratio at 10 m/s and 20 m/s was 4°, which provided the best aerodynamic efficiency. However, increasing the angle of attack to 20° causes a significant decrease in the Cl/Cd ratio, indicating that drag increases faster than lift at high angles, which can lead to aerodynamic instability [6].

This research is expected to provide more accurate guidance in the design of efficient and reliable UAV wings, and make a significant contribution to the development of UAVs with higher performance and operational efficiency [7].

**RESEARCH METHODS**

This research uses a type of three-dimensional numerical simulation method. The software used is Ansys Fluent. Simulations were carried out on NACA 2412 airfoil by varying the angle of attack ( $\alpha = 0^\circ, 4^\circ, 8^\circ, 12^\circ, 16^\circ, 20^\circ$ ) and speed variations of 10 m/s and 20 m/s. The airfoil specifications that will be tested are NACA 2412 which has a Max thickness of 12% at 30% chord. Max camber 2% at 40% chord.

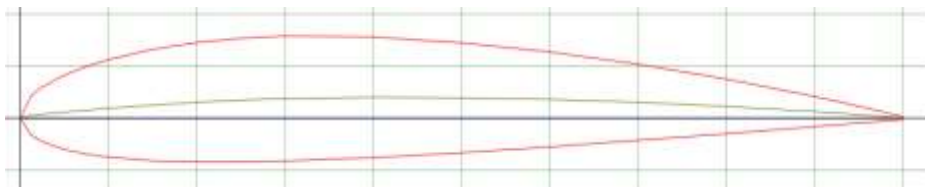


**Fig. 1. NACA 2412 airfoil**

**1. Design Process**

In making the NACA Airfoil 2412 geometry design model using the solidworks application in 2021. The 2021 solidworks application has advantages including: ease of use, the ability to make more accurate designs, connect with other simulation applications, and the renewable solidworks application makes the solidworks application accessible to anyone [8].

**2. Simulation Process**

**a. Preprocessing**

In the initial stage, the design made using the Solidworks application is imported into the Ansys application to simulate the design. The next step is to create a fluid domain for the NACA 2412 Airfoil, this step aims to determine boundary conditions, facilitate data collection, and the value of the required properties. Furthermore, the meshing process which aims to process the stage of the field or volume containing the fluid is divided into small cells.

**b. Processing**

**1. Setup**

When the mesh process is complete, the next step is to enter important information such as material values, boundary conditions, and reference values from the analysis. The first step is to determine the type of fluid flow using the Reynolds number (Re). After that, determine the boundary conditions for turbulence, including providing pressure, load speed, and conditions at the wall, inlet, and outlet. The last step is to input data to run the simulation with variables such as area, density, temperature, velocity, and viscosity [9].

**Table 1. Parameters airfoil NACA 2412**

No.	Parameters	Value
<b>Add local sizing</b>		
1	Body of influence	0.2
2	Facesize body	0.017

Generate the surface mesh		
1	Minimum size	0.017
2	Maximum size	0.4
Add boundary layers		
1	Offset method type	Smooth-transition_1
2	Transition ratio	0.272
3	Number of layers	3
4	Growth rate	1.2
Generate the volume mesh		
1	Solver	Fluent
2	Fill with	Polyhedra
3	Sizing method	Global
4	Growth rate	1.2
5	Max cell length	0.068

**Table 2. parameters input data**

No.	Parameter Input Data	value
1	Fluid flow velocity (V)	varied
2	Temperature (T)	300 K
3	Pressure (P)	1 atm (101325 Pa)
4	Turbulence modul	K- $\omega$ SST
5	Fluid density ( $\rho$ )	1.225 kg/m <sup>3</sup>
6	Viskosity ( $\nu$ )	1.4607 $\times 10^{-5}$ m <sup>2</sup> /s
7	Angle of attack	0°, 4°, 8°, 12°, 16°, 20°

**2. Solution**

In this stage, the method used is a coupled scheme with a second order upwind discretization method to obtain more accurate analysis results. In this study, the report definition is used to calculate the drag coefficient and lift force on the aircraft wing with NACA 2412 airfoil [10]. At this stage, error limits can be used to limit the results of the analysis obtained. After that, to facilitate convergence, hybrid initialization is used. Furthermore, the analysis process is carried out with the number of iterations as needed.

**3. Post Processing**

At this stage the simulation has been completed, after which the simulation is displayed in the form of graphs, images, animations and others. The data obtained include: drag coefficient data, lift coefficient, and pressure coefficient distribution.

**4. Grid Independency Analysis**

To determine the optimum mesh size with the smallest error in CFD analysis, it is necessary to conduct Grid Independency Analysis [7]. In this study, four variations were used with the aim of finding the most optimum mesh value and the smallest error value. The following is the Grid Independency Analysis table used in this research:

**Table 3. Mesh Type**

Mesh Type	Number of MeshCells	Lift Coefficient	Error (%)
Experiment	-	0.105	-
Mesh A	58.347	0.134	27,61
Mesh B	84.664	0.135	28,57
Mesh C	104.653	0.132	25,71
Mesh D	305.202	0.133	26,66

From the table above, the results show that Meshing C gets the smallest error value with a value of 25.71% and becomes a reference and reference for analysis with the following[11] equation:

$$\%error = \left[ \frac{\{(C_l\text{mesh reference}) - (C_l\text{experiment})\}}{(C_l\text{experiment})} \right] \times 100\% \quad (1)$$

In accordance with the standard. If the data does not match, the process of repeating the analysis is carried out until the data is After the data analysis is complete, a recheck is carried out with the aim of ensuring that the data generated is in accordance with the convergent standard. If the analysis results are in accordance with the test standards then proceed with data analysis.

**RESULTS AND DISCUSSION.**

In this study, aerodynamic analysis was conducted on NACA 2412 airfoil applied to an airplane wing. By utilizing ANSYS Fluent software and the CFD Post function, visualization is obtained in the form of velocity contour, pressure contour, and velocity streamline of the analyzed aircraft wing in three-dimensional form. From these results, the drag coefficient (Cd), lift coefficient (Cl), and the relationship between lift and drag coefficients (Cl/Cd) were analyzed.

**a. Analysis of the Effect of Streamline Distribution on NACA 2412**

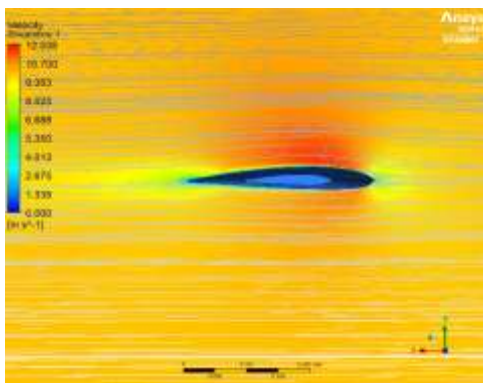


**Fig. 2. Streamline Distribution at AoA 0° speed 10 m/s**

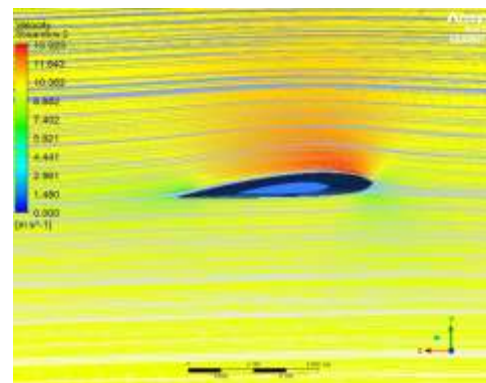


**Fig. 3. Streamline Distribution at AoA 4° speed 10 m/s**

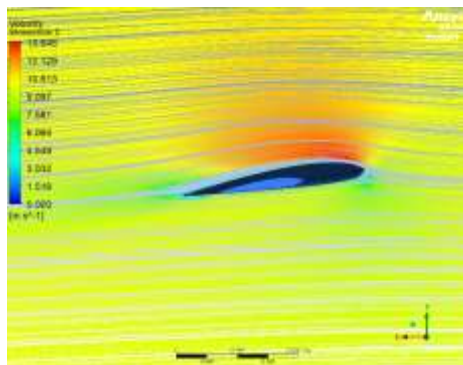


**Fig. 4. Streamline Distribution at AoA 8° speed 10 m/s**

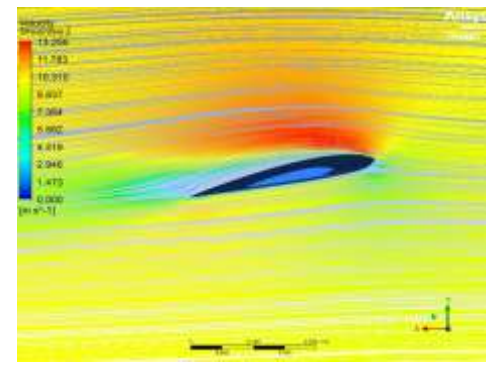


**Fig. 5. Streamline Distribution at AoA 12° speed 10 m/s**

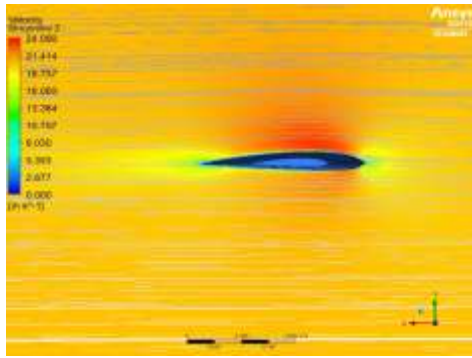


Fig. 6. Streamline Distribution at AoA 0° speed 20 m/s

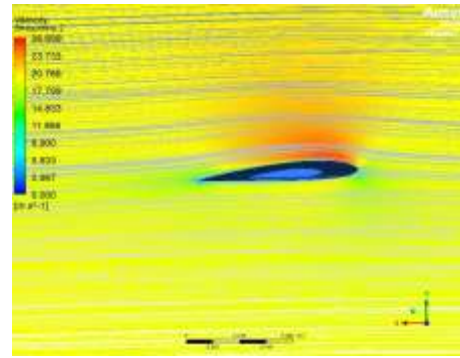


Fig. 7. Streamline Distribution at AoA 4° speed 20 m/s

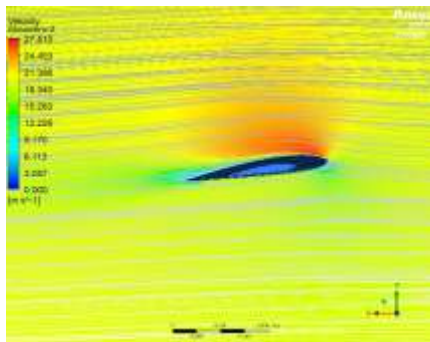


Fig. 8. Streamline Distribution at AoA 8° speed 20 m/s

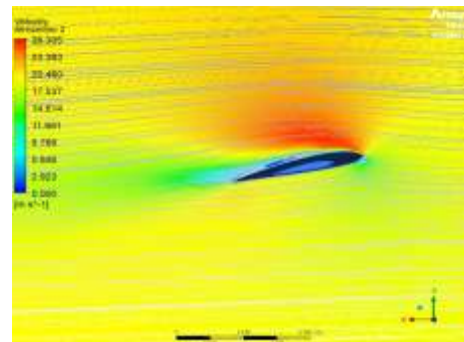


Fig. 9. Streamline Distribution at AoA 12° speed 20 m/s

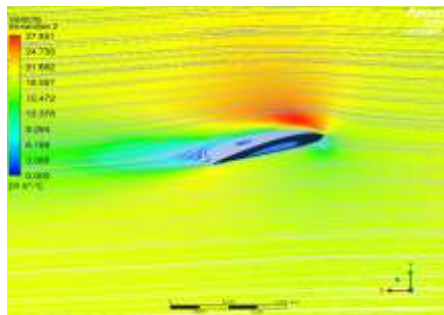


Fig. 10. Streamline Distribution at AoA 16° speed 20 m/s

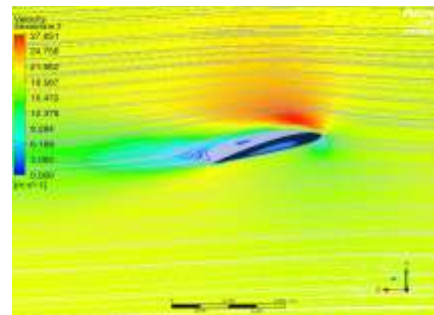


Fig. 11. Streamline Distribution at AoA 20° speed 20 m/s

b. Analysis of the Effect of Pressure Distribution on Airfoil NACA 2412

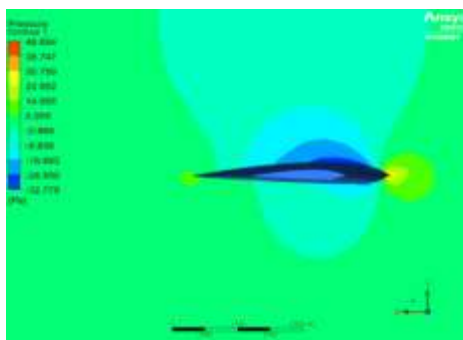


Fig. 12. Pressure distribution at AoA 0° speed 10 m/s

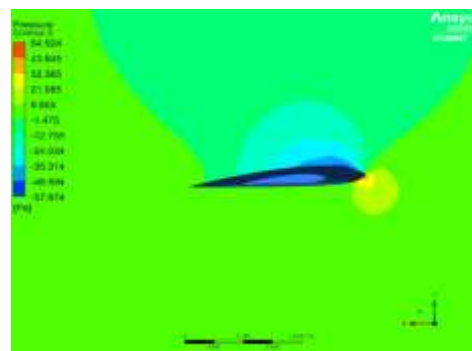


Fig. 13. Pressure distribution at AoA 4° speed 10 m/s

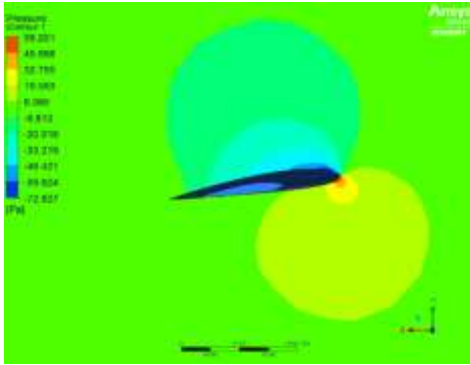


Fig. 14. Pressure distribution at AoA 8° speed 10 m/s

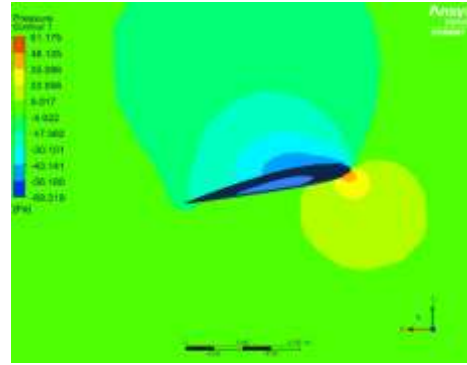


Fig. 15. Pressure distribution at AoA 12° speed 10 m/s

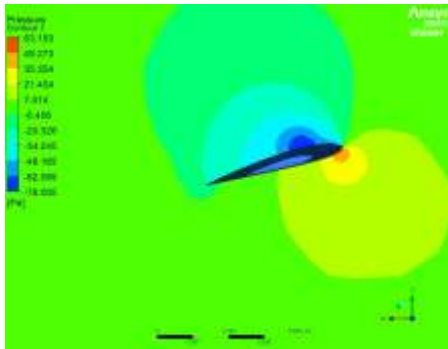


Fig. 16. Pressure distribution at AoA 16° speed 10 m/s

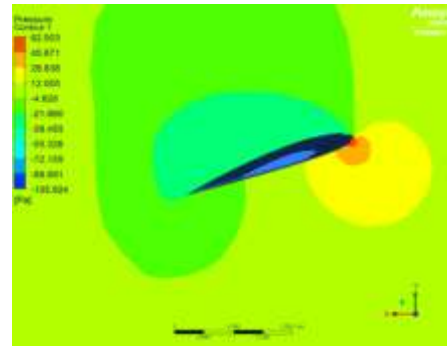


Fig. 17. Pressure distribution at AoA 20° speed 10 m/s

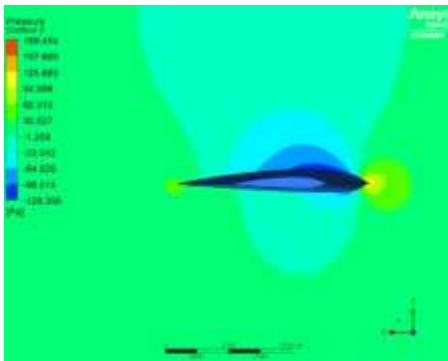


Fig. 18. Pressure distribution at AoA 0° speed 20 m/s

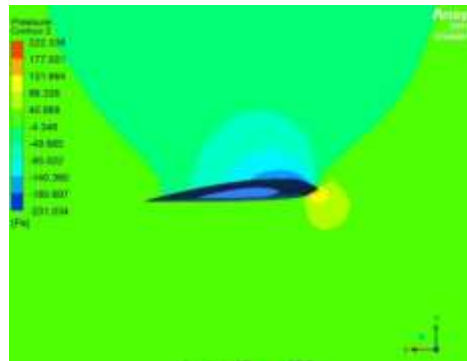


Fig. 19. Pressure distribution at AoA 4° speed 20 m/s

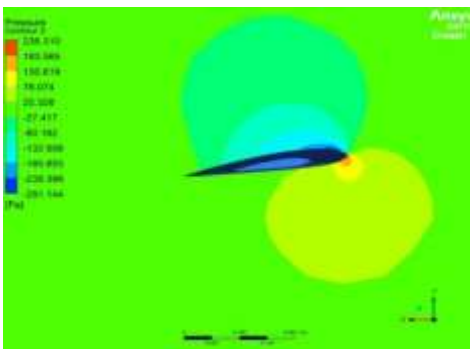


Fig. 20. Pressure distribution at AoA 8° speed 20 m/s

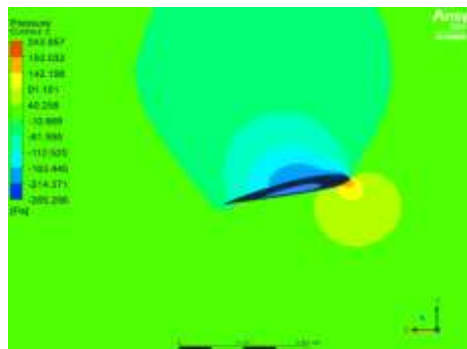


Fig. 21. Pressure distribution at AoA 12° speed 20 m/s

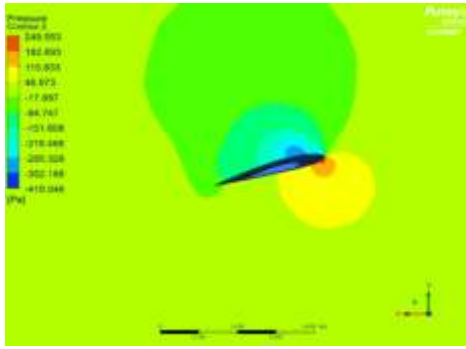


Fig. 22. Pressure distribution at AoA 16° speed 20 m/s

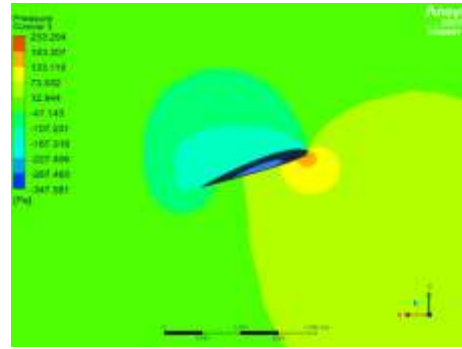


Fig. 23. Pressure distribution at AoA 20° speed 20 m/s

**c. Drag Coefficient Analysis**

The drag coefficient measures the resistance an object experiences when moving through a fluid, such as air. On the wing of a UAV, the drag coefficient affects flight efficiency, where lower drag values reduce air resistance and allow the aircraft to fly more efficiently with lower energy consumption, thereby increasing flight range and duration. Figures 28 and 29 show a comparison of the drag coefficient at angles of attack of 0°, 4°, 8°, 12°, 16°, 20° with velocities of 10 m/s and 20 m/s, respectively.

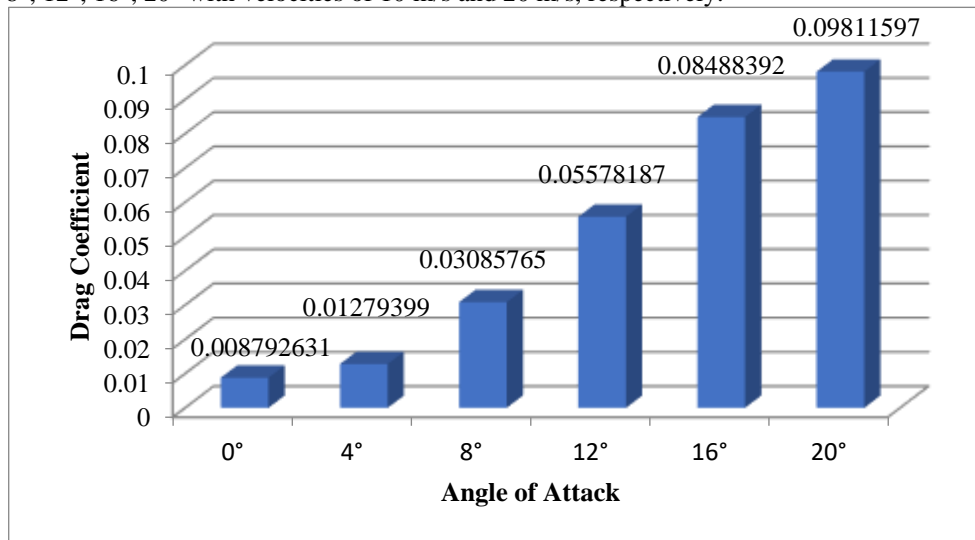


Fig. 24 . Drag Coefficient Value at Attack Angle 0° , 4° ,8° ,12° ,16° ,20° with Speed 10 m/s

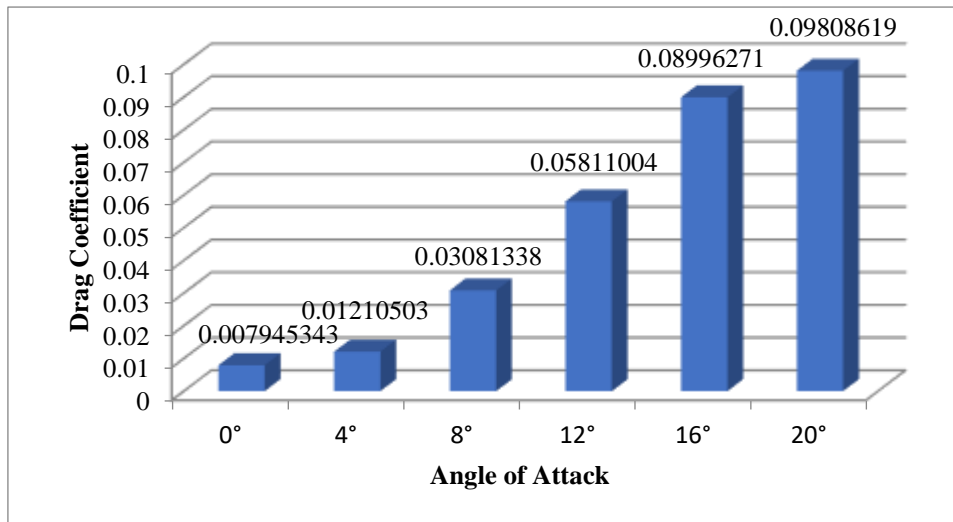


Fig. 25. Drag Coefficient Value at Attack Angle 0°, 4°, 8°, 12°, 16°, 20° with Speed 20 m/s

The graphs in Figures 26 and 27 show the relationship between drag coefficient (Cd) and angle of attack at different speeds. The first graph is for a speed of 10 m/s, and the second graph is for 20 m/s. In both graphs, the value of Cd increases as the angle of attack increases. At 10 m/s, Cd starts from 0.0088 at 0° and increases to 0.0981 at 20°, with a sharp increase after 8°. At 20 m/s, Cd starts from 0.0079 and reaches 0.0981 at 20°, with a similar pattern of increase. In conclusion, increasing the angle of attack causes an increase in Cd at both speeds, although the pattern of increase is similar even though the speed changes from 10 m/s to 20 m/s.

**d. Lift Coefficient**

The coefficient of lift (Cl) indicates the ability of an object, such as an airplane wing or airfoil, to generate lift when exposed to airflow. The Cl value reflects how effectively the shape of the object generates lift based on its shape, angle of attack, and airflow conditions such as speed and density. The higher the Cl, the greater the object's ability to generate lift. Cl is highly dependent on the angle of attack; increasing this angle generally increases Cl up to a certain point before stall occurs. The coefficient of lift is important in the design and analysis of aircraft and other aerodynamic applications because it affects flight efficiency and stability.

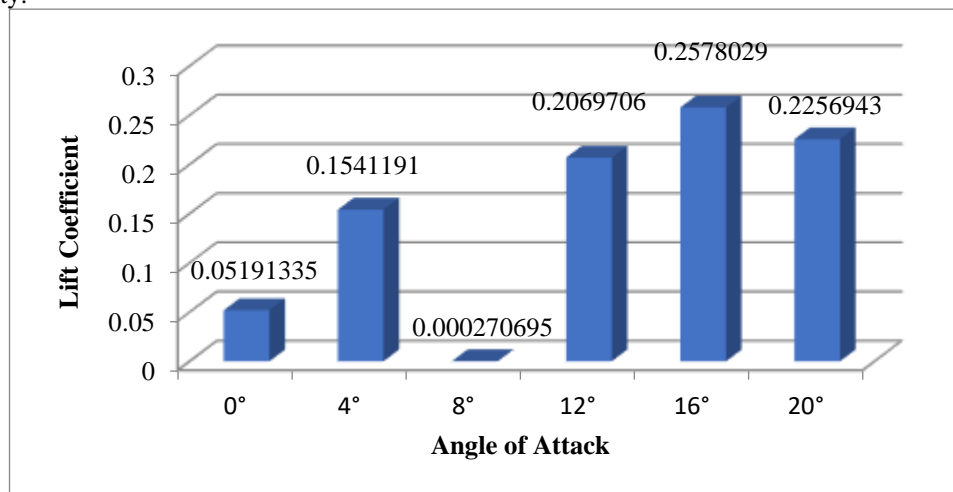
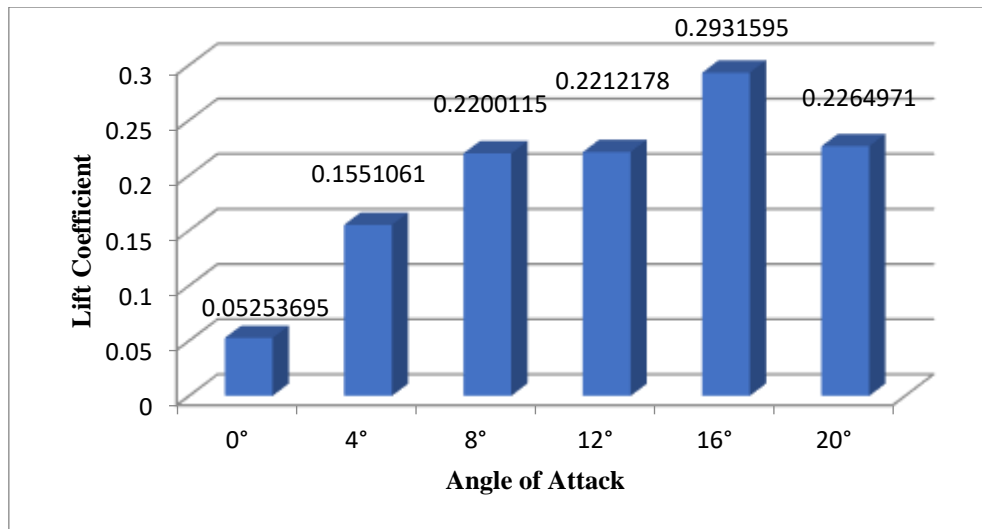


Fig. 26. Lift Coefficient Value at Attack Angle 0°, 4°, 8°, 12°, 16°, 20° with Speed 10 m/s





**Fig. 27. Lift Coefficient Value at Attack Angle 0°, 4°, 8°, 12°, 16°, 20° with Speed 20 m/s**

Figures 29 and 30 show the relationship between lift coefficient (Cl) and angle of attack at 10 m/s and 20 m/s, respectively. Although the patterns at both speeds are similar, the Cl values at each angle of attack differ significantly, with Cl being lower at 10 m/s than at 20 m/s. At 10 m/s, the maximum Cl of 0.2578 occurs at an angle of 16°, while at 20 m/s the maximum Cl reaches 0.2932 at the same angle.

At low angles (0° to 8°), the 10 m/s graph shows a smaller Cl. For example, at an angle of 0°, Cl at 10 m/s is 0.0519, while at 20 m/s, Cl is slightly higher at 0.0525. The difference is more pronounced at an angle of 8°, with Cl of 0.2070 at 10 m/s and 0.2200 at 20 m/s. After the peak at 16°, Cl decreases in both graphs, but at 20°, Cl at 20 m/s (0.2265) remains higher than at 10 m/s (0.2257). Overall, the higher the airflow velocity, the greater the lift coefficient at each angle of attack, in accordance with the aerodynamic principle that increasing flow velocity results in greater lift.

**e. CL/CD Ratio Analysis**

To determine the relationship between angle of attack and coefficient of lift and coefficient of drag at 10 m/s and 20 m/s for NACA 2412 airfoil, it is necessary to calculate the lift-to-drag ratio Cl/Cd. This ratio is obtained by dividing the coefficient of lift by the coefficient of drag. The calculations can be seen in Table 7 and Table 8 below.

**Table 4. Calculation of the lift-to-drag ratio Cl/Cd at a speed of 10 m/s**

Angle of Attack	Lift Coefficient	Drag Coefficient	Ratio
0°	0.05191335	0.008792631	5.9042
4°	0.1541191	0.01279399	12.0462
8°	0.20702706948	0.03085765	0.0088
12°	0.2069706	0.05578187	3.7104
16°	0.2578029	0.08488392	3.0371
20°	0.2256943	0.09811597	2.3002

**Table 5. Calculation of the lift-to-drag ratio Cl/Cd at a speed of 20 m/s**

Angle of Attack	Lift Coefficient	Drag Coefficient	Ratio
0°	0.05253695	0.007945343	6.6123
4°	0.1551061	0.01210503	12.8133
8°	0.2200115	0.03081338	7.1401
12°	0.2212178	0.05811004	3.8068
16°	0.2931595	0.08996271	3.2587
20°	0.2264971	0.09808619	2.3092

A comparison between tables 4 and 5 shows significant variations in aerodynamic efficiency through the lift-to-drag (Cl/Cd) ratio at various angles of attack. At an angle of attack of 0°, the Cl/Cd ratio in table 4 is 5.9042, while in table 5 it increases to 6.6123, indicating the conditions of table 5 result in greater lift with lower drag at low angles. At 4° angle, the aerodynamic efficiency increases with a Cl/Cd ratio of 12.0462 in table 7 and 12.8133 in table 5, where table 5 remains superior.

According to Chen et al. (2018), the highest aerodynamic efficiency usually occurs at low to medium angles, as the airflow remains attached to the airfoil surface without significant flow separation. At 8° angle, a noticeable difference is seen; table 4 shows a decrease in the Cl/Cd ratio to 0.0088, while table 5 remains high at 7.1401, indicating table 5 performs much better at this angle.

Overall, table 5 shows higher Cl/Cd ratios at each angle of attack than table 4, especially at 8°, indicating more efficient aerodynamic performance at each angle of attack tested.

## CONCLUSIONS.

This study has analyzed the aerodynamic characteristics of the NACA 2412 airfoil on the UAV wing using Computational Fluid Dynamics (CFD) simulation through ANSYS Fluent software. Based on the simulation results, it is concluded that the optimal angle of attack to achieve the highest Cl/Cd ratio at 10 m/s and 20 m/s is 4°, where at this angle the combination of lift and drag shows the most optimal aerodynamic efficiency. In addition, increasing the angle of attack to 20° results in a significant decrease in the Cl/Cd ratio, indicating that at high angles of attack the drag force increases faster than the lift force, which can lead to aerodynamic instability. These findings provide important guidance in the selection of optimal angle of attack for UAV wing design, supporting the development of more efficient and stable UAVs under various operational conditions.

## REFERENCES

- [1] Romadhon, A., & Herdiana, D. (2017). Analisis Cfd Karakteristik Aerodinamika Pada Sayap Pesawat Lsu-05 Dengan Penambahan Vortex Generator (Analysis of Cfd Aerodynamic Characteristics At the Wing of Aircraft Lsu-05 With the Addition of Vortex Generator). *Jurnal Teknologi Dirgantara*, 15(1), 45. <https://doi.org/10.30536/j.td.2017.v15.a2518>
- [2] Hidayat, R., & Mardiyanto, R. (2016). Pengembangan Sistem Navigasi Otomatis Pada UAV (Unmanned Aerial Vehicle) dengan GPS (Global Positioning System) Waypoint. *Jurnal Teknik ITS*, 5(2).
- [3] Hidayat, K., Rizaldi, A., Septiyana, A., Ramadiansyah, M. L., & Ramadhan, R. A. (2019). Analisis Pemilihan *Airfoil* Pesawat Terbang Tanpa Awak Lsu-05 Ng dengan Menggunakan Analytical
- [4] Hidayat, M. F. (2016). Analisis Aerodinamika *Airfoil* NACA 0021 Dengan Ansys Fluent. *Universitas 17 Agustus 1945 Jakarta*, 10(2), 83–92.
- [5] Singh, J., Singh, J., Singh, A., Rana, A., & Dahiya, A. (2015). Study of NACA 4412 and Selig 1223 *airfoils* through computational fluid dynamics. *International Journal of Mechanical Engineering*, 2(6), 17–21. <https://doi.org/10.14445/23488360/ijme-v2i6p104>
- [6] Heteyi, C., Molnar, I., & Szlivka, F. (2020). Comparing different CFD software with NACA 2412 airfoil. *Progress in Agricultural Engineering Sciences*, 16(1), 25–40. <https://doi.org/10.1556/446.2020.00004>
- [7] Pane, M. (2023). Nama penulis (cambria 11 italyc) 190 | VANOS. *VANOS Journal Of Mechanical Engineering Education*, 8(2). <http://jurnal.untirta.ac.id/index.php/vanos>
- [8] Saepuddin, A., Chandra Permadi, L., & Heru Adiwibowo, P. (2023). ANALISIS KEKUATAN TABUNG GAS LPG KAPASITAS 12 KG BERBAHAN CAST CARBON STEEL MENGGUNAKAN METODE ELEMEN HINGGA. In *Technology, Education And Mechanical Engineering* (Vol. 4, Issue 1).
- [9] Selvanose, S. M., Marimuthu, S., Awan, A. W., & Daniel, K. (2024). NACA 2412 Drag Reduction Using V-Shaped Riblets. *Eng*, 5(2), 944–957. <https://doi.org/10.3390/eng5020051>
- [10] Novianti, R. D., Hariyadi, S., Putro, S., & Pambudiyatno, N. (n.d.). ANALISIS AERODINAMIKA PENGGUNAAN PLAIN FLAP PADA AIRFOIL NACA 2412. <https://ejournal.poltekbangsby.ac.id/index.ph>